Comparison of methods for the determination of reflective properties of complex composite materials

H.T. Banks[3], Jared Catenacci[2], Amanda Criner[1], M. Morvidone[4], Diana Rubio[4], N. Saintier[5]

***Abstract*— We consider models and methods for the determination of reflective properties that describes the microscopic properties of complex composite materials. Specifically we compare methods for the determination of reflectivity of complex composite materials including the methods based on Efimov's model for permittivity, homogenization approximating techniques and the Prohorov Metric Framework in which one determines a probability distribution for the permittivity. Our ultimate goal is to be able to ascertain material changes (e. g., oxidation) when the materials are subjected to high stress and high temperatures.**

Keywords: Complex composite materials (CCM), Lorentz Model for permittivity, Efimov Model, homogenization, Prohorov Metric Framework

I. INTRODUCTION

Complex materials, including ceramic matrix composites (CMC's), are increasingly used in a wide range of applications including in components of high temperature engines. While these materials offer many positive advantages, the harsh environments the materials are subjected to lead to degradation. In CMC's, air at high temperatures causes formation of oxides. When oxidation occurs the material becomes brittle which leads to catastrophic failure. Applying a mechanical load increases this effect. A cross section of a CMC is shown in Figure 1(a). We propose to investigate using different models in parameter estimation schemes to estimate the reflectance response from a general multilayer dielectric material.

Reflectance spectroscopy can be used to characterize damage and degradation of CMCs [17]. Reflectance data can be obtained from a Fourier Transform Infrared Reflection (FTIR) spectrometer. For an example spectral response, see Figure 1(b). Parameters in composite permittivity models are estimated from reflectance data then related to the degradation of the material. FTIR data are collected over broad sweeps of wavenumbers or frequencies. FTIR data is sensitive to heat treatment and fatigue [18]. We use effective permittivity of dielectric characteristics that describes the microscopic properties of these composite materials.

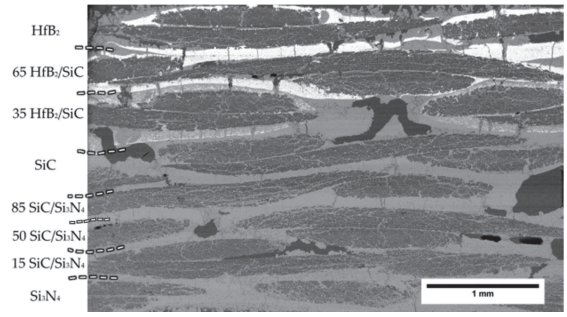

(a)

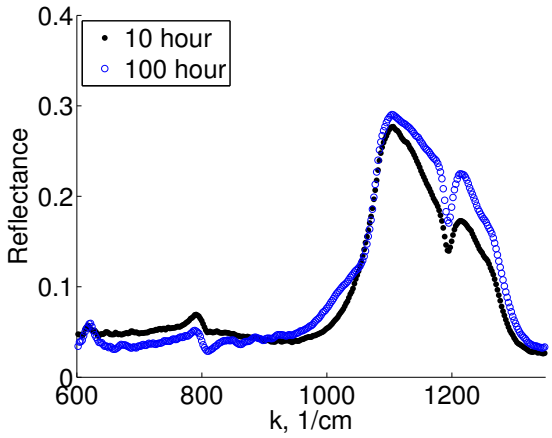

(b)

Fig. 1. (a) A section of a CCM. (b) The reflectance spectra of CMCs that underwent different heat exposures

In this initial attempt to develop results toward the goal of accounting for the heterogeneity of CMCs in their reflectance response, we study the behaviour of the different models on simulated data sets of multilayer materials. We consider several approaches to account for the material complexity and compare these techniques ability to model the reflectance of multilayered materials at different wavelengths.

II. REFLECTANCE OF MULTILAYER MATERIALS

In spectroscopy, data is collected as a function of k (the wave number in units $1/length$), where $k = \omega/(2\pi c)$, ω

*This research was supported in part by the U.S. Air Force Office of Scientific Research under grant AFOSR FA9550-18-1-0457 and in part by SOARD/ AFOSR under Grant FA9550-18-1-0523.

[3]Center for Research in Scientific Computation, North Carolina State University,Raleigh, NC 27695

[2]The Johns Hopkins University Applied Physics Laboratory, Laurel, MD 20723

[1]Structural Materials Division, Materials and Manufacturing Directorate, AFRL/RXCA, Wright-Patterson AFB, Dayton, OH 45433-7750

[4]Centro de Matemática Aplicada - Escuela de Ciencia y Tecnología, Universidad Nacional Gral. San Martín, Buenos Aires, Argentina

[5]Departamento de Matemática, Universidad de Buenos Aires, Buenos Aires, Argentina

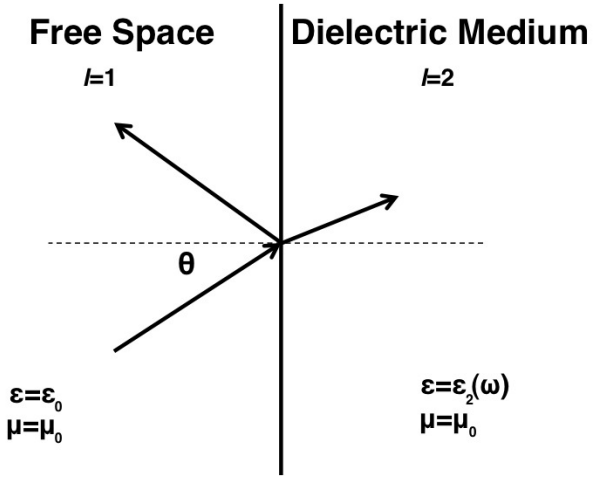

Fig. 2. Schematic of interrogation scheme

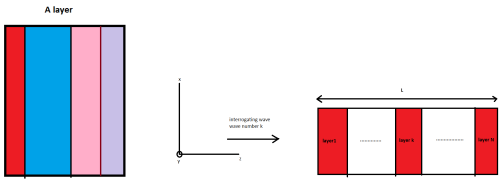

Fig. 3. An example multilayer slab

denotes the interrogating angular frequency, and c is the speed of light in units $length/s$.

We assume that the true material is comprised of a multilayer semi-infinite slab S of total length L in $\mathbb{R}^3$,

$$S = \{(x, y.z) : -\infty < x < \infty, -\infty < y < \infty, 0 \leq z \leq L, \} \tag{1}$$

composed of p infinite vertical layers

$$0 = z_1 < z_2 < ... < z_p = L.$$

The layers have microscopic structure composed of L_p sublayers $S_{L_1}, ..., S_{L_p}$ with sublayer permittivities $\epsilon_1, ..., \epsilon_p$ assumed to be constant. Each sublayer occupies a fraction $\alpha_i \in (0, 1)$ of the layer. This scheme is depicted in Figure 3.

The reflection response Γ_i at the successive interfaces of a multilayer material with M sublayers with refractive indices $n_1, \ldots, n_M$ and elementary reflection coefficients $\rho_1, \ldots, \rho_M$ are given by the recurrence formula (see Orfanidis [25])

$$\Gamma_i = \frac{\rho_i + \Gamma_i e^{2jkl_i}}{1 + \rho_i \Gamma_{i+1} e^{-2jkl_i}} \qquad i = M, M-1, \ldots, 1$$

with $\Gamma_{M+1} = \rho_{M+1}$ and

$$\rho_i = \frac{n_{i-1} - n_i}{n_{i-1} + n_i}, \qquad i = 1, \ldots, M+1.$$

The observed reflectance model has the form

$$R(k) = |\Gamma_1(k)|^2.$$

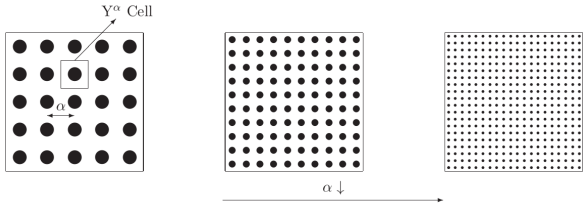

Fig. 4. The homogenization scheme

The total observation model for the simulated data is given by

$$Y_j = R(k_j; G_0, \theta_0) + \nu_j; \ j = 1, .., n \tag{2}$$

where Y_j is the observed random variable, G_0 the "true" probability measure, θ_0 are "true" parameters, k_j sampling wavenumber, and ν_j is random measurement error (assumed i.i.d. with mean 0 and constant variance). For this initial evaluation, we did not include noise to avoid confounding the comparison of the models. The corresponding reflectivity curves are plotted in black and labeled "data" in all of the figures below.

III. HOMOGENIZATION

Techniques based on homogenization [4], [15], [16] assume that the material undergoing interrogation occupies the domain Ω that is made of a *periodic micro-structure*. Thorough discussion of the details of these techniques is well beyond the scope of this work. These details can be found in [4], [15], [16] and references therein.

For the homogenization models here, we assume a periodic structure with elementary micro-structure with size $\alpha > 0$. The reference cell Y is repeated to form the periodic structure that occupies the sample domain Ω. Homogenization approximations are derived through a limiting process on the periodic structure as depicted Figure 4. This process result in limit equations for the homogenized structure.

The closed form solutions given in Cioranescu and Paulin [16], and Banks et. al. [4] assume that $k^{-1} >> \alpha$ where k is the wavenumber of the interrogating signal. We use a numerically discretized versions of the formulas from equations (36)-(38) in [4].

IV. PROBABILITY MEASURE DEPENDENT SYSTEMS-MAXWELL'S EQUATIONS

The probability measures to represent the materials' heterogeneity relies on Maxwell's equations in a complex, heterogeneous material (see [7] and the extensive electromagnetics references therein including [23], [24] for further details). Maxwell's equations are given by

$$\nabla \times E = -\frac{\partial B}{\partial t}, \qquad \nabla \times H = \frac{\partial D}{\partial t} + J, \tag{3}$$

$$\nabla \cdot D = \rho, \qquad \nabla \cdot B = 0, \tag{4}$$

where E is the total electric field, H is the magnetic field, D is the electric flux density (also called the electric displacement), B is the magnetic flux density, and ρ is the density of charges in the medium. The constitutive relations

are material and wavelength dependent. Here, we use the constituitive relations

$$D = \epsilon_0 E + MP \quad B = \mu_0 H + M \quad J = J_c + J_s \tag{5}$$

with macroscopic electric polarization MP, magnetization M, conduction current density J_c, source current density J_s, electric current density J, dielectric permittivity of free space ϵ_0, and the magnetic permeability of free space μ_0.

A general constitutive polarization law is given by

$$MP(t,x) = [\hat{g} * E](t,x) = \int_0^t \hat{g}(t-s,x)E(s,x)ds,$$

where $\hat{g}$ is the polarization susceptibility kernel or dielectric response function (DRF), and x is the spatial coordinate. For complex composite materials, one needs multiple material parameters in some kind of distribution. The model becomes

$$MP(t,x;P) = \int_\Psi mp(t,x;\psi)dP(\psi),$$

where Ψ is a set of possible material parameters ψ, $P \in \mathbb{P}(\Psi)$ where $\mathbb{P}(\Psi)$ is the set of probability distribution functions on Ψ, and mp is the microscopic polarization. It is important to note that MP represents the *macroscopic* polarization, as opposed to the *microscopic polarization* mp which describes polarization at the molecular level and is given by

$$mp(t,x;\psi) = \int_0^t \hat{g}(t-s,x;\psi)E(s,x)ds. \tag{6}$$

The macroscopic polarization MP is integrated over the microscopic (at the molecular level) polarization mp (just as the macroscopic electric field E is integrated over the microscopic electric field e in derivations in [23], [24]). This integration over an underlying distribution is a type of aggregate dynamics.

Assuming no fixed charges ($\rho = 0$) and nonmagnetic material ($M = 0$), equations (3)–(4) become

$$\begin{aligned} \nabla \times E &= -\frac{\partial}{\partial t}(\mu_0 H) \\ \nabla \times H &= \frac{\partial}{\partial t}\left[\epsilon_0 E + \int_0^t G(t-s,x;P)E(s,x)ds\right] + J \\ \nabla \cdot D &= 0 \\ \nabla \cdot H &= 0 \end{aligned} \tag{7}$$

where $P \in \mathbb{P}(\Psi)$ and

$$G(t-s,x;P) = \int_\Psi \hat{g}(t-s,x;\psi)dP(\psi).$$

The dielectric permittivities are modeled to obtain the resultant reflectance model which is then used characterize CCMs. In FTIR modeling, the permittivity is modeled by considering the polarization which results from the displacement of electrons from equilibrium under the effect of an applied electromagnetic field. The resulting constitutive equations from Maxwell's equations are given by

$$D(t,x) = \epsilon_0\, \epsilon_r E(t,x) + P_R(t,x), \qquad (t,x) \in (0,T) \times \Omega$$

where D is electric flux density, ϵ_r is complex permittivity, E is the electric field and P_R is the electric polarization. In general, the refractive index n is related to complex permittivity ϵ by

$$\epsilon = n^2.$$

A. Lorentz Model for permittivity

The Lorentz model for the complex relative permittivity with multiple oscillators is given by

$$\hat{\varepsilon}(k) = \varepsilon_\infty - \sum_{j=1}^{N} \frac{S_j}{k^2 - ik/\tau_j - k_{0_j}^2},$$

where N is the number of oscillators, ϵ_∞ is the relative permittivity of the medium at infinite frequency, τ_j is the relaxation time of the jth oscillator, k_{0_j} is the resonant wavenumber of the jth oscillator, and S_j is the intensity of the jth oscillator. The intensities can be parameterized by $S_j = \Delta\epsilon_{0_j} k_{0_j}^2$ where $\sum_{j=1}^{N} \epsilon_{0_j} = \epsilon_s - \epsilon_\infty$ and ϵ_s is the relative permittivity of the medium at zero frequency (or static dielectric constant). The resultant parameter set θ is

$$\theta = (\epsilon_\infty, \{k_{0_j}, \tau_j, S_j\}_{j=1,..,N}),$$

where $\theta \in \Theta \subset R^{3N+1}$ and Θ is assumed to be compact.

B. Efimov Model for permittivity

The Efimov model [19], [20], [21], [22] formulates a **Gaussian probability density function** in the model for the relative permittivity given by

$$\hat{\varepsilon}(k) = \varepsilon_\infty - \sum_{j=1}^{N} \frac{S_j}{c_j} \int_0^\infty \frac{exp(-(x-k_{0_j})^2/2\sigma_j^2)}{k^2 - ik/\tau_j - x^2} dx,$$

where N is the number of oscillators, ϵ_∞ is the relative permittivity of the medium at infinite frequency, τ_j is the relaxation time of the jth oscillator, k_{0_j} is the resonance number of the jth oscillator, σ_j is the parameter for the Gaussian function, and S_j is the intensity of the jth oscillator. For this model, the parameter set is given by

$$\theta = (\epsilon_\infty, \{k_{0_j}, \tau_j, \sigma_j, S_j\}_{j=1,..,N})$$

where $\theta \in \Theta \subset R^{4N+1}$ and Θ is assumed to be compact.

C. Probability Measure Framework (PMF) for permittivity

The PMF approach, like the Efimov formulation, considers a probability distribution of dielectric parameters but does not specify the form of the pdf. Rather, one considers approximation methods in estimation where the quantity of interest is a probability distribution. Assume we have a parameter dependent system with model responses $x(t,q)$ describing the populations of interest. The model observations are given by a set of expected values $\{y_l\}$

$$E[x_l(q) \mid P] = \int_Q x_l(q)dP(q) \tag{8}$$

for the model $x_l(q) = x(t_l, q)$ with an unknown probability distribution P describing the distribution of parameters q

over the population. One then uses data to estimate the distribution P from a given family $\mathbb{P}(Q)$.

The form of the measurement noise ν_j in the data generating model (equation (2)) indicates an ordinary least squares (OLS) problem. One could use other approaches but comparison between algorithms for estimating parameters is not the focus of this work. Following the OLS framework, we seek to minimize

$$J(P) = \sum_l |E[x_l(q)|P] - y_l|^2 \tag{9}$$

over $P \in \mathbb{P}(Q)$.

Even for simple dynamics for x_l, this leads to an infinite dimensional optimization problem so approximations that lead to computationally tractable schemes are necessary. To yield finite dimensional sets $\mathbb{P}^M(Q)$ over which to minimize $J(P)$, methods are chosen so that $\mathbb{P}^M(Q) \to \mathbb{P}(Q)$ as $M \to \infty$ in some sense (see [1], [13]). We use the Prohorov metric [3], [5] which metrizes the weak star convergence of measures to assure approximation results. We use this framework to model the permittivity function given by

$$\hat{\varepsilon}(k) = \varepsilon_\infty - (\varepsilon_s - \varepsilon_\infty) \int \frac{k_0^2}{k^2 - ik/\tau - k_0^2} dG(k_0).$$

The relative permittivity of the medium at zero frequency and "infinite" frequency are denoted ϵ_s and ϵ_∞, respectively. The relaxation time is given by τ, and the probability measure is given by G. The probability measure defined over a specified set of wavenumbers $\mathcal{K} \subset \mathbb{R}$. The probability measure is the family of probability functions over the wavenumber set $\mathcal{K}$ ($G \in \mathbb{P}(\mathcal{K})$). The probability distribution function G is approximated by piece-wise linear splines with 40 nodes uniformly spaced in $[700, 1400]$. We estimate $\theta = (\epsilon_\infty, \epsilon_s, w_1, ..., w_{N_s})$ where w_i are the weights of the splines used to approximate the probability measure $G(k)$. We seek $(\hat{G}, \hat{\theta}) \in \mathbb{P}(\mathcal{K}) \times \Theta$ where

$$(\hat{G}, \hat{\theta}) = \arg\min J(G, \theta), \tag{10}$$

and the argmin is taken over $\mathbb{P}(\mathcal{K}) \times \Theta$. The cost function $J(G, \theta)$ is defined by

$$J(G, \theta) = \sum_{j=1}^{n} \left(R(k_j; G, \theta) - y_j\right)^2. \tag{11}$$

The simulated data is given by

$$y_j = R(k_j; G_0, \theta_0) \quad j = 1, ..n, \tag{12}$$

for a chosen (G_0, θ_0) based on our experience with data from heated CCM's.

V. NUMERICAL RESULTS

In the numerical simulations, the slab has total length $L = 0.01$cm. The slab has 20 layers. Each layer has $p = 4$ equally spaced sublayers. The size of the resultant microstructure is $\alpha = \frac{L}{20} = 5 \times 10^{-4}$. Each of the 4 sublayers occupies $\frac{1}{4}$ of a layer. The simulated data is given by $y_j = R(k_j, \theta)$, $j = 1, .., 100$. We estimate the parameters θ for each model by minimizing the least square errors

$$\sum_{j=1}^{100} |R(k_j) - R(k_j, \theta)|^2.$$

First, we use data with 100 uniformly spaced values in the wave number interval $[700, 1400]$. Though this is the wavenumber range of interest, see Figure 1, we will also consider data for smaller wavenumbers k (with $k^{-1} \gg \alpha$) where homogenization is more appropriate [4], [16].

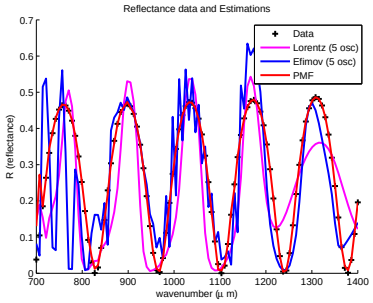

Fig. 5. Reflectance values for $k \in [700, 1400]\text{cm}^{-1}$ with refractive index vector $[1.38, 2.38, 2, 3]$ and sublayers proportions $[1/4, 1/4, 1/4, 1/4]$.

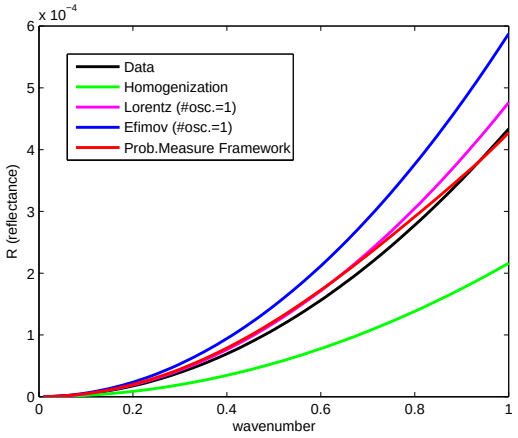

Fig. 6. Reflectance for $k \in [0.0001, 1]\mu\text{m}^{-1}$ with refractive index vector $[1.38, 2.38, 2, 3]$ with sublayer proportions $[1/4, 1/4, 1/4, 1/4]$.

Lorentz	0.3658
Efimov	0.3827
PMF	0.0616

TABLE I
RELATIVE ERRORS FOR THE REFLECTANCE VALUES IN FIGURE 5.

We include an LSQ approach for the "effective permittivity". These results were obtained by using an OLS fit using a model which assumes $P_R(t.x) = constant$ in the basic polarization law $D(t, x) = \epsilon_0 \epsilon_r E(t, x) + P_R(t, x)$.

VI. Conclusions

For wavenumbers $k > 0.5$, the **PMF** model approximates reflectance from a multi-layered system best. As the

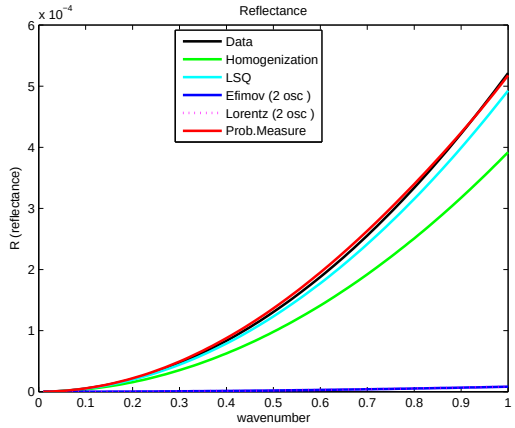

Fig. 7. Reflectance for $k \in [0.01, 1]$ with refractive index vector $[1.38, 2.38, 2, 3]$ and sublayer proportions $[1/4, 1/4, 1/4, 1/4]$.

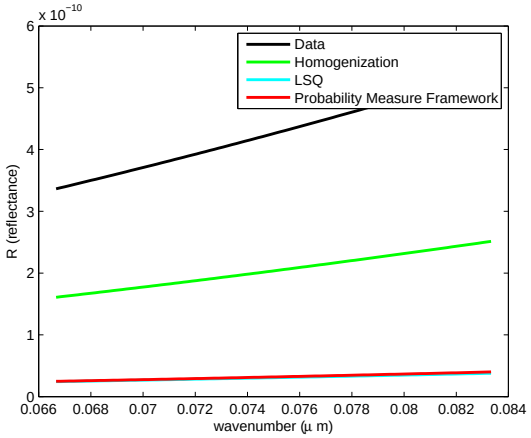

Fig. 8. Reflectance values for length $L = 10^{-4}$ μ m, refractive index vector $[1.3, 2.4, 2, 3]$ and sublayer proportions $[1/4, 1/4, 1/4, 1/4]$.

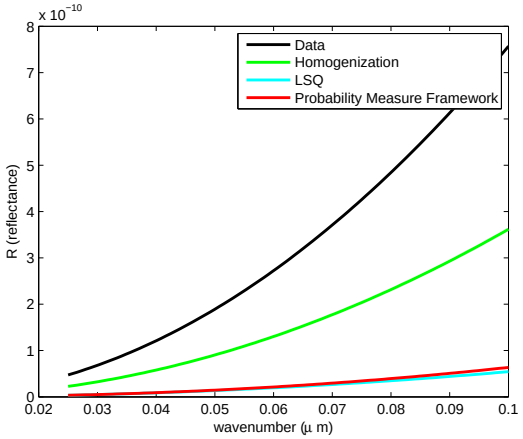

Fig. 9. Reflectance values for $k \in [0.025, 0.1]\mu\text{m}^{-1}$ with length $L = 1e-4\mu$m, refractive index vector $[1.3, 2.4, 2, 3]$, and sublayer proportions $[1/4, 1/4, 1/4, 1/4]$.

Homogenization	0.5019
Lorentz	0.0982
Efimov	0.3550
PMF	0.0530

TABLE II

RELATIVE ERRORS IN REFLECTANCE VALUES IN FIGURE 6.

Homogenization	0.24834
Lorentz	0.98374
Efimov	0.98417
PMF	0.01977
LSQ	0.05501

TABLE III

RELATIVE ERROR FOR REFLECTANCE VALUES IN FIGURE 7.

wavenumbers decrease **homogenization** better approximates reflectance from a multi-layered system. This work establishes the performance of different approaches and models of a multi-layered material. Further work needs to be done to fully characterize the performance of these different models given variations in the layer structure, sublayer structure, refractive indices and wavenumbers. Future efforts will continue to account for material heterogeneity in the analysis of reflectance data from CMCs, such as incorporating different geometries to account for surface roughness and material coatings. Analysis of experimental data from composite materials will be included in future efforts.

ACKNOWLEDGMENTS

This research was supported in part by the U.S. Air Force Office of Scientific Research under grant AFOSR FA9550-18-1-0457 and in part by SOARD/AFOSR under Grant FA9550-18-1-0523.

REFERENCES

[1] H.T. Banks, A Functional Analysis Framework for Modeling, Estimation and Control in Science and Engineering, Chapman and Hall/CRC Press, Boca Raton, FL, 2012.

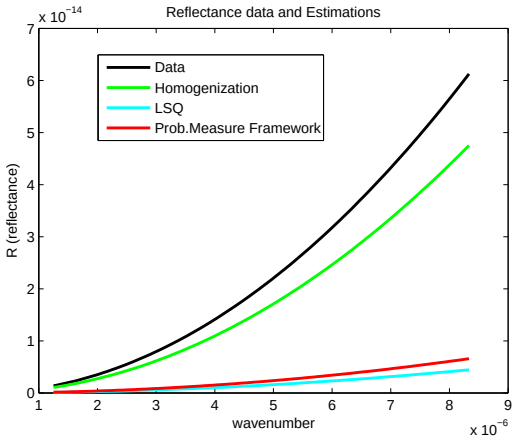

Fig. 10. Reflectance values for $k \in [1.2510^{-6}, 8.310^{-6}]$ with refractive index vector $[1.3, 2.4, 2, 3]$, and sublayer proportions $[1/4, 1/4, 1/4, 1/4]$.

Homogenization	0.52189
PMF	0.92502
LSQ	0.92814

TABLE IV

RELATIVE ERRORS OF THE REFLECTANCE VALUES IN FIGURE 8.

Homogenization	0.62459
PMF	0.81661
LSQ	0.91836

TABLE V

RELATIVE ERRORS FOR THE REFLECTANCE VALUES IN FIGURE 9.

Homogenization	0.22428
PMF	0.89263
LSQ	0.92744

TABLE VI

RELATIVE ERRORS IN REFLECTANCE VALUES IN FIGURE 10.

[2] H. T. Banks, John E. Banks, Natalie G. Cody, Mark S. Hoddle, and Annabel E. Meade, Population model for the decline of Homalodisca vitripennis (Hemiptera: Cicadellidae) over a ten-year period, J. Biological Dynamics, 13 (2019), 422–446.

[3] H.T. Banks and K.L. Bihari, Modelling and estimating uncertainty in parameter estimation,Inverse Problems, 17 (2001), 95–111.

[4] H.T Banks, V.A. Bokil, D. Cioranescu, N.L. Gibson, G. Griso, and B. Miara, Homogenization of periodically varying coefficients in electromagnetic materials, CRSC-TR05-05, January, 2005; *J. Scientific Computing*, **28** (2006), 191–221.

[5] H.T. Banks, D.M. Bortz, G.A. Pinter and L.K. Potter, Modeling and imaging techniques with potential for application in bioterrorism, CRSC-TR03-02, January, 2003; Chapter 6 in Bioterrorism: Mathematical Modeling Applications in Homeland Security, (H.T. Banks and C. Castillo-Chavez, eds.), Frontiers in Applied Math, FR28, SIAM, Philadelphia, PA, pp. 129–154, 2003.

[6] H.T. Banks, L.W.Botsford, F. Kappel and C. Wang, Modeling and estimation in size structured population models , LCDS/CCS Rep. 87-13, March, 1987, Brown Univ.; Proc. 2nd Course on Math. Ecology (Trieste, December, 1986), World Scientific Press, Singapore (1988), 521-541.

[7] H.T. Banks, M.W. Buksas and T. Lin, *Electromagnetic Material Interrogation Using Conductive Interfaces and Acoustic Wavefronts*, SIAM FR **21**, Philadelphia, 2002.

[8] H.T. Banks and J. Catenacci. Aggregate data and the Prohorov metric framework: efficient gradient computation. Applied Math Letters, 56:1-9, 2016.

[9] H. T. Banks, J. Catenacci, and A. Criner. Quantifying the degradation in thermally treated ceramic matrix composites. The 17th International Symposium on Applied Electromagnetics and Mechanics (ISEM2015); Intl J. of Applied Electromagnetics and Mechanics, 52 (2016) 3–24.

[10] H.T. Banks, J. Catenacci, S. Hu, Asymptotic properties of probability measure estimators in a nonparametric model. SIAM/ASSA. Journal of uncertainty quantification, 3 (1), pp. 417-433, 2015.

[11] H.T. Banks, J. Catenacci, and S. Hu. Estimation of distributed parameters in permittivity models of composite dielectric materials using reflectance. Journal of Inverse and Ill-Posed Problems, 23(5):491-509, 2015.

[12] H. T. Banks, K. B. Flores, I. G. Rosen, E. M. Rutter, Melike Sirlanci, and W. Clayton Thompson, The prohorov metric framework and aggregate data inverse problems for random PDEs, Communications in Applied Analysis, 22:415–446, 2018.

[13] H. T. Banks, Shuhua Hu, and W. C. Thompson, *Modeling and Inverse Problems in the Presence of Uncertainty,* Taylor and Frances Publishing, Chapman and Hall/CRC Press, Boca Raton, FL, 2014.

[14] H. T. Banks and W. C. Thompson, Random delay differential equations and inverse problems for aggregate data problems, Eurasian J. Mathematical and Computer Applications, 6, No. 4 (2018), 4–16.

[15] V.A. Bokil, H.T. Banks, D.Cioranescu, and G. Griso, A multiscale method for computing effective parameters of composite electromagnetic materials with memory effects. Quarterly of Applied Mathematics, 76 (2018), 713-738.

[16] D. Cioranescu and J. S. J. Paulin, Homogenization of Reticulated Structures (Applied Mathematical Sciences, Vol 136), Springer, New York, 1999.

[17] A.K. Criner, Christine Henry, Megan Imel, Derek King, and Ming Chen, Handheld Fourier Transform Infrared Spectroscopic Characterization of Ceramic Matrix Composites, Materials Evaluation, 75: 953-964, 2017.

[18] Cooney, A.T., Flattum-Riemers, R.Y. and Scott, B.J., 2011, June. Characterization of material degradation in ceramic matrix composites using infrared reflectance spectroscopy. In AIP Conference Proceedings (Vol. 1335, No. 1, pp. 950-955). AIP.

[19] A.M. Efimov, Optical Constants of Inorganic Glasses, CRC press, Boca Raton, Florida, 1995.

[20] A.M. Efimov, Quantitative IR spectroscopy: Applications to studying glass structure and properties, Journal of Non-Crystalline Solids, 203 (1996), 1–11.

[21] A.M. Efimov, Vibrational spectra, related properties, and structure of inorganic glasses, Journal of Non-Crystalline Solids, 253 (1999), 95–118.

[22] A.M. Efimov and E. G. Makarova, Dispersion equation for the complex dielectric constant of vitreous solids and dispersion analysis of their reflection spectra, Fiz. Khim.Stekla (Journal of Applied Spectroscopy), 11, (1985), 385.

[23] R.S. Elliot, *Electromagnetics: History, Theory, and Applications*, IEEE Press, New York, 1993.

[24] J.D. Jackson, *Classical Electrodynamics*, J. Wiley & Sons, New York, 1975.

[25] S.J. Orfanidis, Electromagnetic Waves and Antennas, ECE Department, Rutgers University, 94 Brett Road, Piscataway, NJ 08854-8058, downloadable print copy, 2016.